## Plant Physiology®

# Transcription factors VviWRKY10 and VviWRKY30 co-regulate powdery mildew resistance in grapevine

Min Zhou, 1,2,† Hongyan Wang, 1,2,† Xuena Yu, 1,2 Kaicheng Cui, 1,2 Yang Hu, 1,2 Shunyuan Xiao, 3,4 and Ying-Qiang Wen, 1,2,\*

- 1 State Key Laboratory of Crop Stress Biology for Arid Areas, College of Horticulture, Northwest A&F University, Yangling 712100, Shaanxi, China
- 2 Key Laboratory of Horticultural Plant Biology and Germplasm Innovation in Northwest China, Ministry of Agriculture and Rural Affairs, Yangling 712100, Shaanxi, China
- 3 Institute for Bioscience and Biotechnology Research, University of Maryland, Rockville, MD 20850, USA
- 4 Department of Plant Science and Landscape Architecture, University of Maryland, College Park, MD 20742, USA

\*Author for correspondence: wenyq@nwsuaf.edu.cn (Y.-Q.W.)

<sup>†</sup>These authors contributed equally to this work.

The author responsible for distribution of materials integral to the findings presented in this article in accordance with the policy described in the Instructions for Authors (https://academic.oup.com/plphys/pages/General-Instructions) is Ying-Qiang Wen (wenyq@nwsuaf.edu.cn).

#### **Abstract**

Grapevine (*Vitis vinifera*) is an economically important fruit crop worldwide. The widely cultivated grapevine is susceptible to powdery mildew caused by *Erysiphe necator*. In this study, we used CRISPR-Cas9 to simultaneously knock out *VviWRKY10* and *VviWRKY30* encoding two transcription factors reported to be implicated in defense regulation. We generated 53 *wrky10* single mutant transgenic plants and 15 *wrky10* wrky30 double mutant transgenic plants. In a 2-yr field evaluation of powdery mildew resistance, the *wrky10* mutants showed strong resistance, while the *wrky10* wrky30 double mutants showed moderate resistance. Further analyses revealed that salicylic acid (SA) and reactive oxygen species contents in the leaves of *wrky10* and *wrky10* wrky30 were substantially increased, as was the ethylene (ET) content in the leaves of *wrky10*. The results from dual luciferase reporter assays, electrophoretic mobility shift assays and chromatin immunoprecipitation (ChIP) assays demonstrated that VviWRKY10 could directly bind to the W-boxes in the promoter of SA-related defense genes and inhibit their transcription, supporting its role as a negative regulator of SA-dependent defense. By contrast, VviWRKY30 could directly bind to the W-boxes in the promoter of ET-related defense genes and promote their transcription, playing a positive role in ET production and ET-dependent defense. Moreover, VviWRKY10 and VviWRKY30 can bind to each other's promoters and mutually inhibit each other's transcription. Taken together, our results reveal a complex mechanism of regulation by VviWRKY10 and VviWRKY30 for activation of measured and balanced defense responses against powdery mildew in grapevine.

#### Introduction

Grapevine (*Vitis* sp.) is an important fruit crop with high nutritional and economic values and a long history of cultivation in the world (Jaillon et al. 2007). However, the widely cultivated European grapevine species *Vitis vinifera* is highly susceptible to powdery mildew caused by *Erysiphe necator*, resulting in serious losses in growth and yield (Gadoury et al. 2012; Gao et al. 2016; Hu et al. 2018). Therefore, it is

necessary and urgent to create disease-resistant grapevine through breeding and novel transgene technologies.

Rapid and massive transcriptional reprogramming events are often associated with plant-pathogen interactions, in which transcription factors (TFs) play important roles (Tsuda and Somssich 2015). Among the large family of TFs in plants, WRKY TFs are mainly involved in responding to various biological stresses (Eulgem and Somssich 2007; Jiang et al. 2017). In Arabidopsis thaliana, AtWRKY18 and

AtWRKY40 are negative regulators of powdery mildew resistance by inhibiting the expression of cytochrome P450 family 71 polypeptide (CYP71A13), the enhanced disease susceptibility 1 (EDS1) and peptidylarginine deiminase 4 (PAD4). The double mutant wrky18wrky40 and triple mutant wrky18wrky40wrky60, but not the wrky18, wrky40, and wrky60 single mutants, are substantially more resistant to powdery mildew than the wild type (WT), indicating that AtWRKY18 and AtWRKY40 have partially redundant functions in Arabidopsis (Xu et al. 2006; Shen et al. 2007; Pandey et al. 2010). The Xanthomonas type-III effector XopS interacts with and inhibits proteasomal degradation of CaWRKY40a, preventing the plant from properly activating defense genes and the expression of key genes required for stomatal closure, making it easier for pathogens to enter the pepper (Capsicum annuum) leaves (Raffeiner et al. 2022). Rosa hybrida (Rh)WRKY13, which is an ortholog of AtWRKY40, protects rose petals against Botrytis cinerea infection by binding to the promoter region of the cytokinin degradation 3 (RhCKX3) and the abscisic acid insensitive 4 (RhABI4), inhibiting their expression in rose petals, increasing CK content and reducing ABA response (Liu et al. 2022).

Further, it was reported that the target genes of AtWRKY18 and AtWRKY40 under flg22 treatment included multiple hormone pathways, including salicylic acid (SA) and ethylene (ET) (Birkenbihl et al. 2017). It is well known that WRKYs can regulate hormone pathways and play important roles in plant immunity. CaWRKY27 enhances the resistance of *Nicotiana benthamiana* to *Ralstonia solanacearum* by regulating SA, jasmonic acid (JA), and ET-mediated signaling pathways (Dang et al. 2014). AtWRKY55 regulates leaf senescence and pathogen resistance by directly binding to the W-boxes of respiratory burst oxidase homologue D (*RBOHD*), isochorismate synthase 1 (*ICS1*), cytosolic enzyme avrPphB susceptible 3 (*PBS3*), and senescence-associated gene 13 (*SAG13*), activating their expression and integrating ROS and SA pathways in Arabidopsis (Wang et al. 2020).

It was reported that WRKY10 and -30 in grapevine, as homologous genes of AtWRKY18 and -40, also are involved in regulating the interaction between grapevine and pathogens (Guo et al. 2014; Ma et al. 2021). Overexpression of Vitis amurensis WRKY10 in A. thaliana and in V. vinifera increases resistance to B. cinerea (Wan et al. 2021). Due to different naming rules, some studies refer to VviWRKY30 as VviWRKY40. Plasmopara viticola effector PvRXLR111 interacts with VviWRKY40 and improves its stability to suppresses the immune response of grapevine to P. viticola (Ma et al. 2021). Besides the above studies, it remains to be seen whether VviWRKY10 and -30 regulate resistance to powdery mildew in grapevine, and whether they also have partial functional redundancy as do AtWRKY18 and -40 in Arabidopsis.

In this study, two mutants in grapevine, wrky10 and wrky10wrky30, were obtained and used for characterizing their potential role in resistance to powdery mildew. It was found that wrky10 showed strong resistance and wrky10wrky30 showed moderate resistance. Moreover, the resistance of the

mutants was due to significant increase of SA and ROS levels in wrky10 and wrky10wrky30 compared to WT plants. Interestingly, wrky10 but not wrky10wrky30 exhibited highlevel ET accumulation. By DLUC, EMSA, and ChIP-qPCR, we proved that VviWRKY10 inhibits enhanced disease susceptibility 5-2 (EDS5-2), pathogenesis-related protein 1 (PR1), pathogenesis-related protein 5 (PR5), and respiratory burst oxidase homologue D 2 (RBOHD2) expression via directly targeting their promoters. We also showed that VviWRKY30 binds to the promoters of 1-aminocyclopropane-1carboxylate synthase 3 (ACS3) and ACS3 like (ACS3L) and promote their expression, and VviWRKY10 and VviWRKY30 mutually inhibit each other's gene expression. Combined, our results demonstrate distinctive roles of VviWRKY10 and VviWRKY30 in modulating grapevine's defense responses against powdery mildew through transcriptional regulation of different genes involved in the SA, ET, and ROS pathways.

#### **Results**

### Identification and characterization of VviWRKY10 and VviWRKY30 in grapevine

To investigate whether VviWRKY10 and VviWRKY30 are responsive to powdery mildew, cDNA of these two genes was prepared from leaf tissues of the susceptible V. vinifera cv. Cabernet Sauvignon. Analysis of the deduced protein sequences showed that both VviWRKY10 and VviWRKY30 had a highly conserved WRKY domain and a typical C<sub>2</sub>H<sub>2</sub> zinc finger motif (Supplementary Fig. S1). The phylogenetic tree was constructed by using the protein sequences of VviWRKY10, VviWRKY30, and WRKYs related to Arabidopsis, apple, pepper, and rice. The results showed that VviWRKY30 was closely related to MdWRKY40, clustered with CaWRKY40, AtWRKY40, and VviWRKY10 into one subfamily (Fig. 1A). Gene expression of VviWRKY10 and VviWRKY30 in "Cabernet Sauvignon" inoculated with powdery mildew E. necator NAFU1 (En. NAFU1) (Gao et al. 2016) was detected by reverse transcription quantitative PCR (RT-qPCR). The transcript level of VviWRKY10 had a rapid increase from 0 to 24 hours postinoculation (hpi), and peaked at 24 hpi, which was 8.7-fold than at 0 hpi (Fig. 1B). Differing from VviWRKY10, expression of VviWRKY30 increased from 24 to 48 hpi, peaking at 48 hpi with a 71-fold increase relative to its expression at 0 hpi (Fig. 1C). Hence, in terms of gene transcription, VviWRKY10 responded to powdery mildew infection earlier than VviWRKY30.

To determine if VviWRKY10 and VviWRKY30 have nuclear localization like most TFs, we constructed the 35S: *VviWRKY10-eGFP* (enhanced Green Fluorescent Protein) and 35S:*VviWRKY30-eGFP* fusion expression vectors and transiently expressed in leaves of *N. benthamiana*, using 35S:*AtH2B-mCherry* as the nuclear localization marker. As shown in Fig. 1D, VviWRKY10 and VviWRKY30 had typical nuclear localization, which was also verified by overlapping localization with the marker protein.

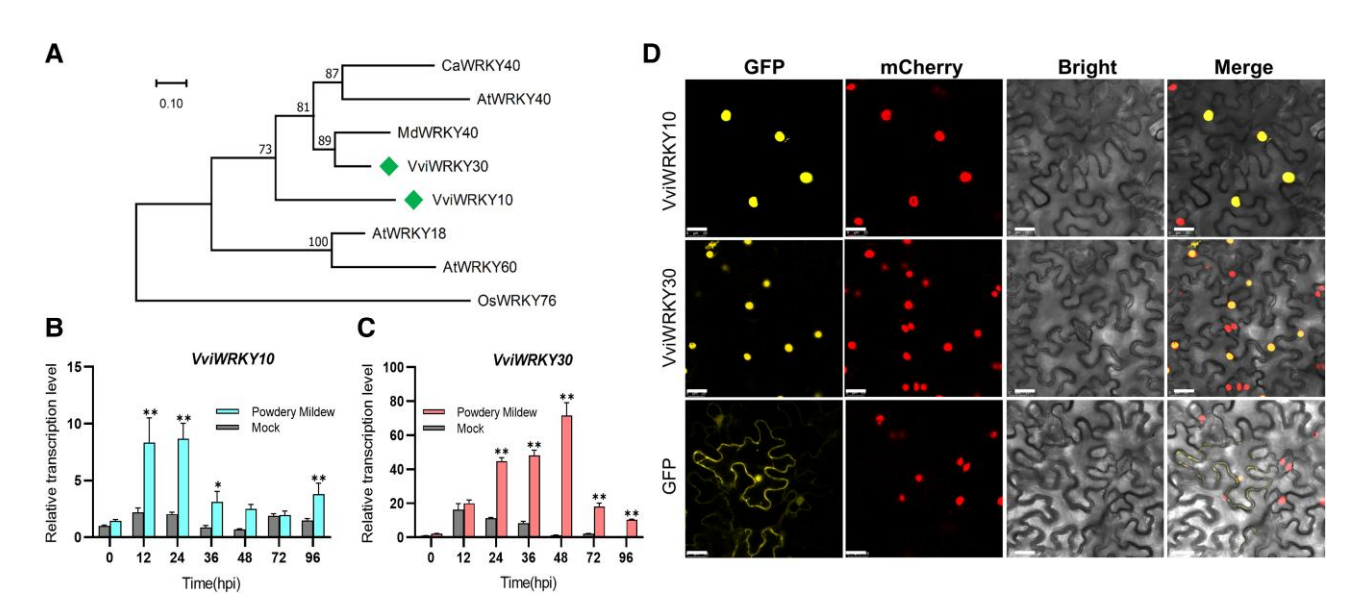


**Figure 1.** Phylogenetic and expression analysis of VviWRKY10 and VviWRKY30. **A)** Phylogenetic analysis of WRKY proteins in V.vinifera (Vvi), A.thaliana (At), O.sativa (Os), Malus domestica (Md), and C.annuum (Ca). The diamond squares represent the WRKY proteins in V.vinifera. The phylogenetic tree was constructed by MEGA-X. The scale bar represents 0.1 substitutions per site. **B, C)** Relative transcript levels of VviWRKY10 (**B)** and VviWRKY30 (**C)** post-E.necator NAFU1 inoculation. VviACTIN7 ( $XM_002282480.4$ ) gene was used as an endogenous control. **D)** Subcellular localization of VviWRKY10 and VviWRKY30. AtH2B:mCherry served as the nuclear marker. Bars, 25  $\mu$ m. Each data point represents the mean  $\pm$  standard deviation of three biological replicates, and asterisks indicate significant difference compared with 0 hpi (two-way ANOVA, \*\*P < 0.01; \*P < 0.05).

### CRISPR-Cas9-mediated mutagenesis of VviWRKY10 and VviWRKY30

It was reported that the Atwrky18/40 double and Atwrky18/ 40/60 triple mutants but not the Atwrky18, Atwrky40, or Atwrky60 single mutants were almost fully resistant to powdery mildew (Shen et al. 2007; Pandey et al. 2010). Therefore, we constructed a dual-target vector targeting VviWRKY10 and VviWRKY30 simultaneously in grapevine. The two target regions were located on the first exon of VviWRKY10 and the third exon of VviWRKY30, respectively (Fig. 2A). Two small guide (sg) RNAs were integrated into an intermediate vector to form an expression box, which was eventually reassembled into a GFP-tagged vector (Fig. 2B). The vector was transformed into "Cabernet Sauvignon" proembryo masses (PEM) by Agrobacterium tumefaciens-mediated transformation, and the transgene-positive plants were reported by GFP signals in the subculture (Supplementary Fig. S2, A and B). The results indicate that GFP fluorescence remains stable in the tissue-cultured plantlets even after transplanting them into a greenhouse (Supplementary Fig. S2, C and D).

A total of 111 regenerated plantlets were obtained, of which 91 were GFP positive and the transformation efficiency was 81.98%. Sixty-eight mutants were obtained from 91 GFP-positive plants, including 53 wrky10 mutants and 15 wrky10wrky30 double mutants with an editing efficiency of 74.73% (Table 1, Supplementary Fig. S3A). However, no wrky30 mutants were obtained despite repeated transformation efforts. Among wrky10 mutants, different types of mutations were identified. They included biallelic, heterozygous, and chimeric mutations as shown in lines 34, 45, 66, 70, and 13; among the wrky10wrky30 double mutants, there are

several different types of combinatory mutations in the two target genes. For example, the mutations in line 1 is homozygous for *VviWRKY10* and chimeric for *VviWRKY30*; the mutations in line 10 and line 59 are biallelic for *VviWRKY10* and homozygous or chimeric for *VviWRKY30*; the mutations in line 3 and line 26 are the heterozygous for *VviWRKY10* and chimeric for *VviWRKY30* (Figs. 2C and 3A, Supplementary Figs. S3B and S4, Table 1).

### Mutated VviWRKY10 and/or VviWRKY30 affect the growth in grapevine

For line 1 in which VviWRKY10 is homozygously edited (knocked out), compared with WT, it showed narrow leaves and low lignification of stems, and died before transplanting to the matrix (Fig. 3A, Table 1). Except for the nonviable plants such as line 1, other gene-edited and control lines were cultured in a growth chamber for 2 mo, then transplanted to the greenhouse and observed for over 2 yr (2021–22). In the growth chamber, the average plant height of wrky10wrky30 was lower than that of WT, but there was no statistically significant difference between wrky10 mutants and WT (Fig. 3, B and D). After growing in the greenhouse for 2 yr, WT plants grew normally, with a survival rate of 83.72%; however, among the wrky10 mutants, all the biallelic mutants died, the heterozygously and chimerically edited plants grew weakly with a total survival rate of 52.83%; among the wrky10wrky30 double mutants, three VviWRKY10 biallelically edited plants survived, of which two were VviWRKY30 homozygously edited and one was VviWRKY30 chimerically edited, and the remaining double mutants grew poorly, with a total survival rate of 53.33% (Table 1). In the greenhouse, all the plant height of mutants

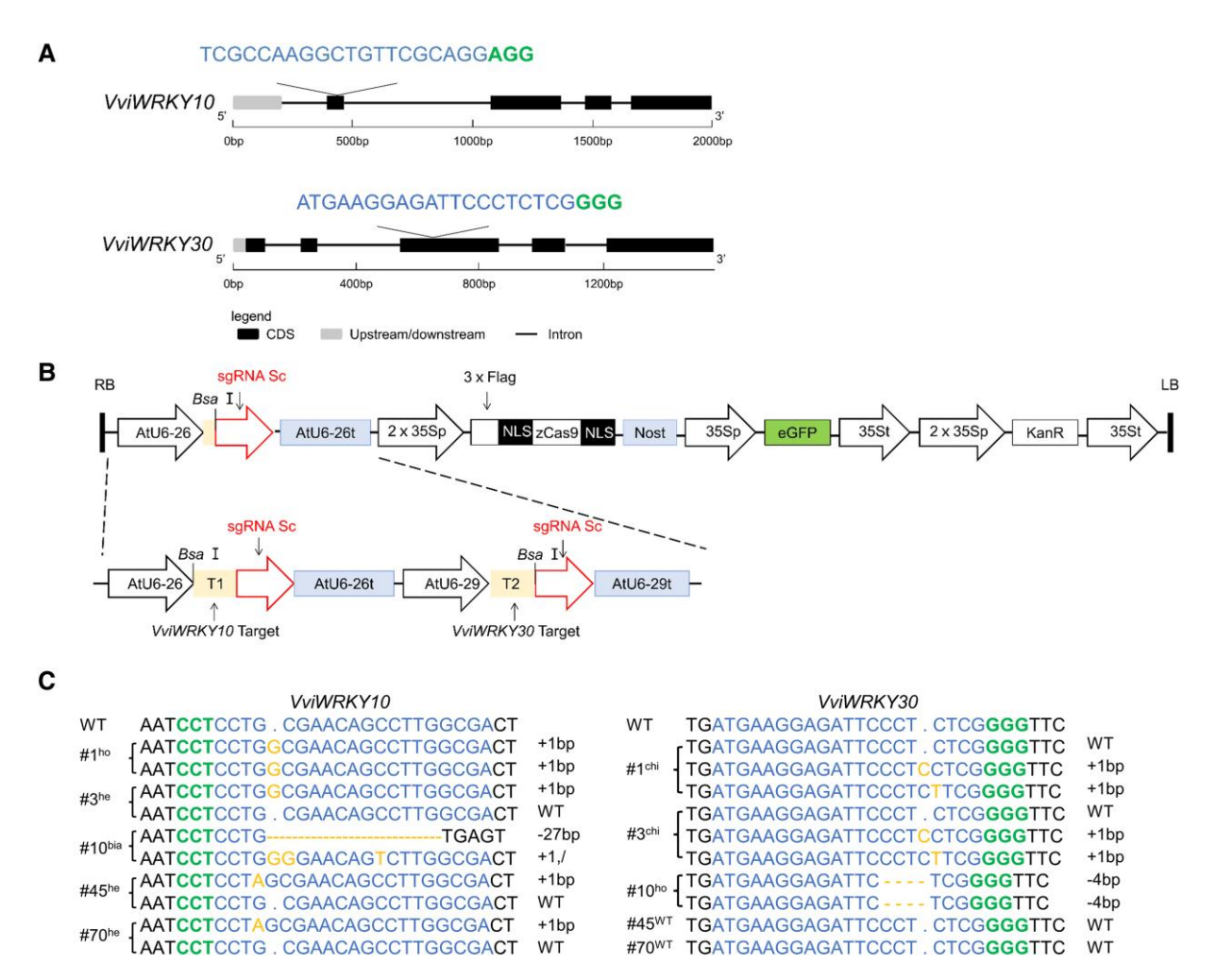


**Figure 2.** Construction of knockout vector and detection of edited plants. **A)** The position of the target sites in *VviWRKY10* and *VviWRKY30*. CDS, coding sequences. Black boxes indicate CDS, gray boxes upstream or downstream untranslated regions, and horizontal lines indicate introns. **B)** Schematic diagram of an expression cassette of intermediate vector and T-DNA region of pKSE401-GFP expression vector. sgRNA sc, sgRNA scaffold. **C)** Different types of CRISPR-Cas9-induced mutations were detected in *VviWRKY10* and *VviWRKY30* genes of mutants. Type of mutations with "–" for deletion, "+" for insertion, "/" for substitution. ho Homozygous, he Heterozygous, his Biallelic, chi Chimeric. The orange, green, and blue letters indicate mutation sequences. PAM sequences, and target sequences, respectively.

was significantly lower than that of WT (Fig. 3, C and E). Furthermore, compared with WT plants, ABA content in *wrky10* mutants was significantly decreased, whereas IAA content in *wrky10wrky30* mutants was significantly increased (Supplementary Fig. S5).

# wrky10 single and wrky10wrky30 double mutants display differential responses to powdery mildew infection

To further study the impact of mutations in *VviWRKY10* and *VviWRKY30* on powdery mildew resistance, some regenerated plants including two *wrky10* lines (lines 45 and 70) and two *wrky10wrky30* lines (lines 3 and 10) were selected infection tests with *En.* NAFU1, with nonedited WT as control. The inoculated leaves were stained with trypan blue, 3,3'-diaminobenzidine (DAB), and aniline blue, as shown in Fig. 4A, trypan blue staining indicated hypersensitive response (HR)-like cell death induced by *En.* NAFU1 in *wrky10* lines,

less in wrky10wrky30 line 3, while almost no cell death in VviWRKY30 homozygously edited line 10 and WT; DAB staining and aniline blue staining showed large areas of H<sub>2</sub>O<sub>2</sub> accumulation and callose deposition in wrky10 lines, less in wrky10wrky30 lines, and barely in WT. Compared with WT plants, the average areas showing H2O2 and callose deposition in wrky10 increased 55- and 165-fold; conversely, the total hyphal length was reduced to 60% of the WT level. As for wrky10wrky30 mutant line 10, despite a 20- and 57-fold increase in areas positive for H<sub>2</sub>O<sub>2</sub> and callose deposition, there was no significant difference in total hyphal length between line 10 and WT (Fig. 4, B to D). These results indicate that wrky10 single mutants displayed strong resistance, whereas the wrky10wrky30 double mutant line 3 showed only weaker resistance and line 10 with no oblivious resistance.

To further explore the gene functions of VviWRKY10 and VviWRKY30, 35S:VviWRKY10-eGFP, and 35S:VviWRKY30-eGFP

Table 1. Summary of genome editing results in regenerated plants

Regenerated plants	Mutation type	Lines	Line ID		Total lines/
			Dead lines	Surviving lines	Survival rate
Wild type (WK10 <sup>-</sup> / WK30 <sup>-</sup> )	Nontransgenic	20	#31, #64, #109	#9, #18, #33, #37, #40, #43, #49, #57, #61, #62, #78, #89, #91, #95, #96, #97, #98	43/83.72%
	Nonedited	23	#63, #76, #79, #93	#8, #19, #20, #21, #25, #29, #30, #44, #50, #65, #68, #71, #84, #86, #87, #90, #101, #103, #111	
wrky10 (WK10 <sup>+</sup> / WK30 <sup>-</sup> )	WK10 <sup>bia</sup>	3	#34, #38, #41	None	53/52.83%
	WK10 <sup>he</sup>	37	#2, #4, #5, #35, #39, #60, #66, #75, #80, #83, #88, #106, #107, #108, #110	#6, #7, #11, #12, #22, #23, #32, #45, #46, #47, #48, #51, #52, #53, #58, #70, #73, #74, #85, #94, #104, #105	
	WK10 <sup>chi</sup>	13	#13, #15, #16, #17, #24, #100, #102	#14, #42, #56, #67, #77, #99	
wrky10wrky30 (WK10 <sup>+</sup> / WK30 <sup>+</sup> )	WK10 <sup>ho</sup> /WK30 <sup>chi</sup>	1	#1	None	15/53.33%
	WK10 <sup>bia</sup> /WK30 <sup>ho</sup>	3	#36	#10, #55	
	WK10 <sup>bia</sup> /WK30 <sup>chi</sup>	3	#28, #54	#59	
	WK10 <sup>he</sup> /WK30 <sup>chi</sup>	3	#69	#3, #26	
	WK10 <sup>chi</sup> /WK30 <sup>chi</sup>	5	#27, #72,	#81, #82, #92	

WK10: VviWRKY10; WK30: VviWRKY30.

Nontransgenic: GFP negative, unedited; Nonedited: GFP positive, unedited.

<sup>+:</sup> Edited, -: Unedited, ho: Homozygous, he: Heterozygous, bia: Biallelic, chi: Chimeric.

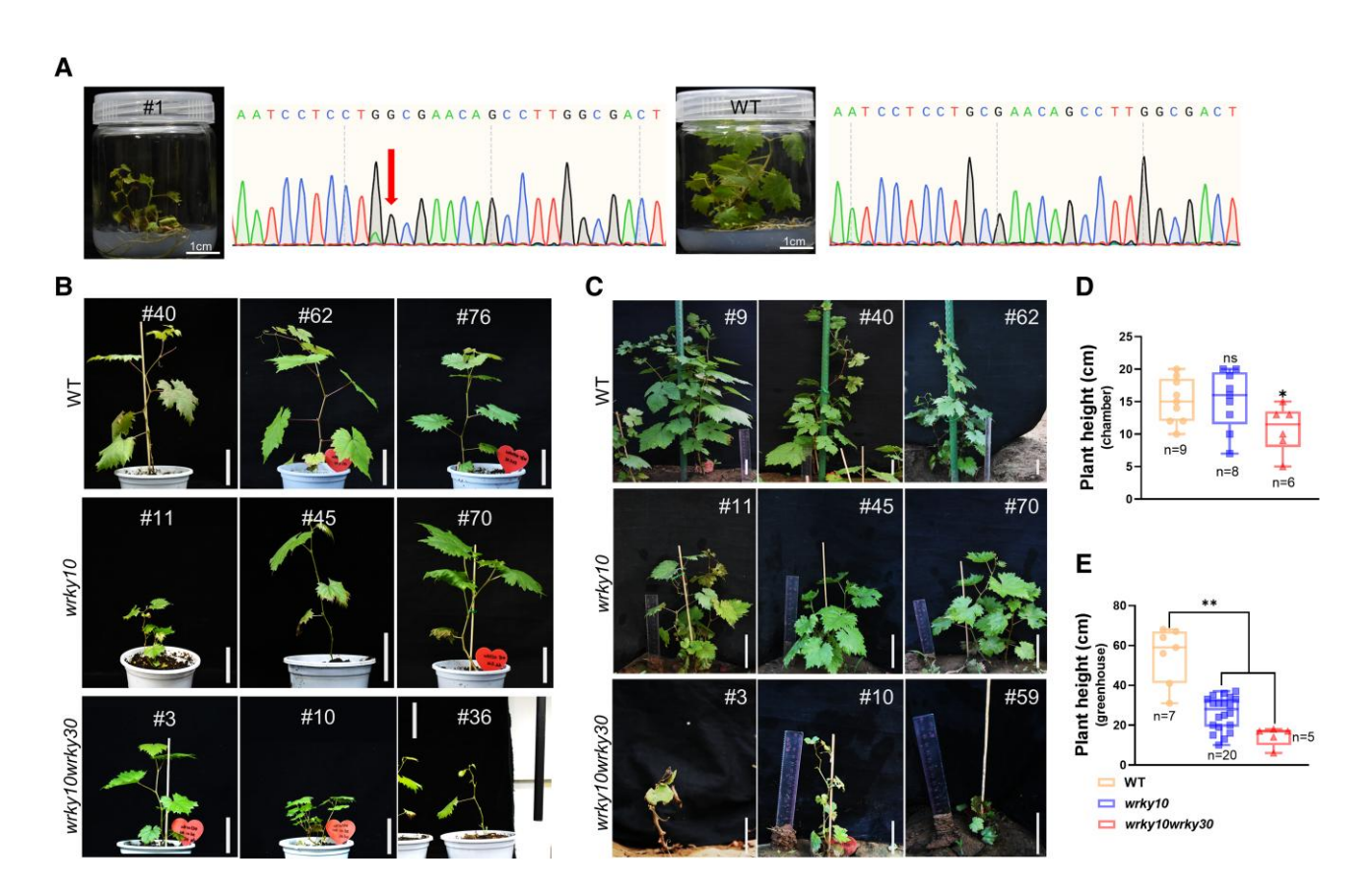


**Figure 3.** CRISPR-Cas9-mediated mutagenesis of *VviWRKY10* and *VviWRKY30* regulate growth in grapevine. **A)** Phenotype and sequencing chromatograms of #1 and WT, insertion G was indicated by arrow. **B, C)** Phenotypes of WT and mutants grown in chamber **(B)** and greenhouse **(C)**. Bars, 5 cm. **D, E)** Plant height of WT and mutants grown in chamber **(D)** and greenhouse **(E)**. Each data point represents the mean  $\pm$  standard deviation of multiple biological replicates, and asterisks indicate significant difference compared with WT (Box hinges: 75% quantile, median, 25% quantile, respectively, from top to bottom. Whiskers: lower or upper hinge represents the minimum or maximum value. Student's *t* test, \*\*P < 0.01; \*P < 0.05; ns = no significant difference).

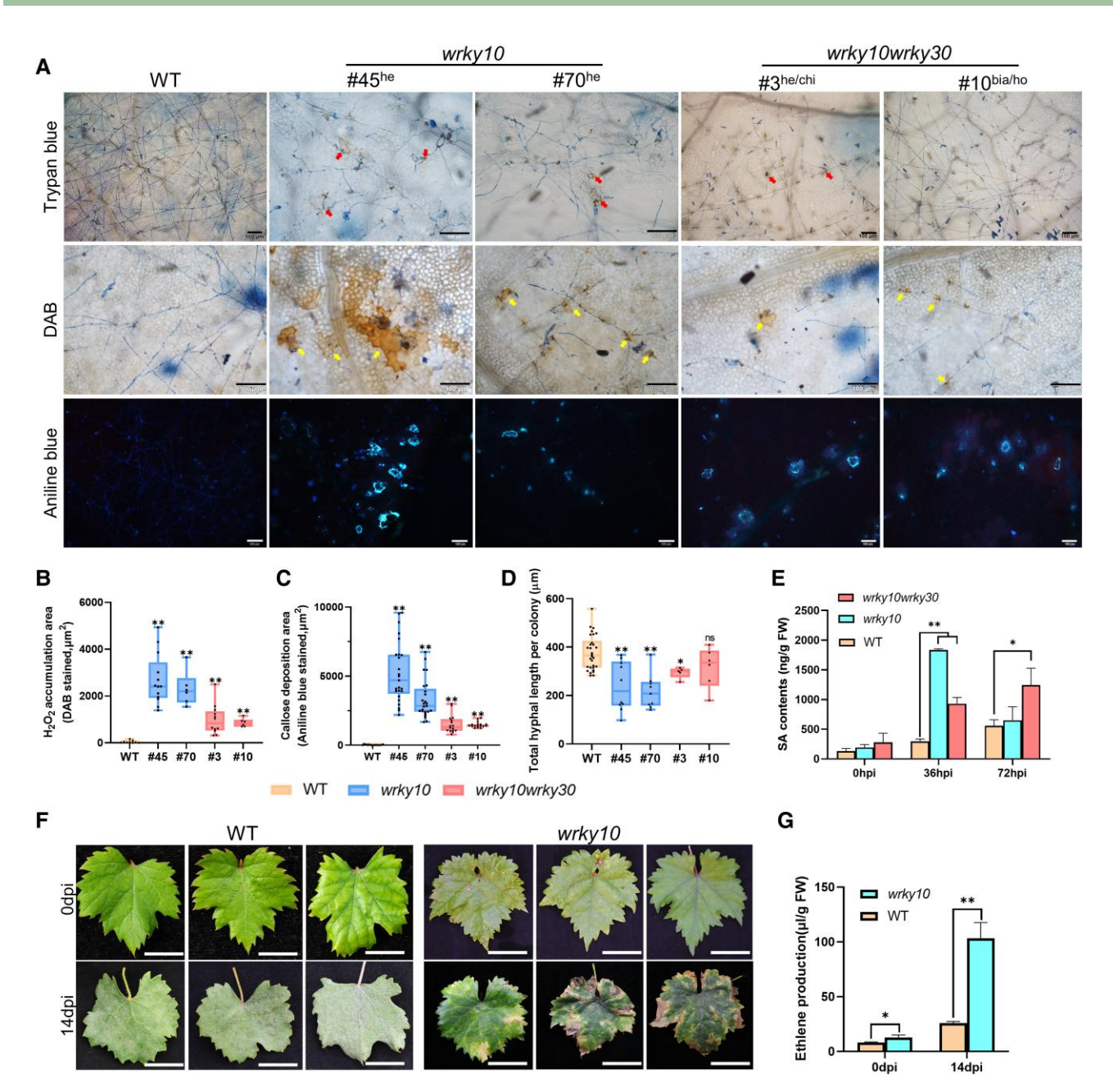


**Figure 4.** VviWRKY10 and VviWRKY30 regulate powdery mildew resistance in grapevine. **A)** Trypan blue, DAB, and aniline blue staining of WT, wrky10, and wrky10wrky30 leaves after inoculation with En. NAFU1. The cell death was indicated with arrows in the first row, accumulation of  $H_2O_2$  were indicated with arrows in the second row. Bars, 100 μm. DAB, 3,3′-diaminobenzidine. **B to D)** Quantification of  $H_2O_2$  accumulation (**B**), callose deposition (**C**), and hyphal length (**D**). Average hyphal length per colony at 3 dpi, accumulation of  $H_2O_2$  and callose at 5 dpi. Box hinges: 75% quantile, median, 25% quantile, respectively, from top to bottom. Whiskers: lower or upper hinge represents the minimum or maximum value. **E)** SA contents of WT and mutants. Leaves used for detection were collected from WT, wrky10 and wrky10wrky30 lines at 36 and 72 hpi. SA, salicylic acid. **F)** Phenotypes of WT and wrky10 leaves at 0 and 14 dpi. Bars, 2 cm. **G)** Ethylene production of detached leaves per 36 h which were collected from WT and wrky10 lines at 0 and 14 dpi. Each data point represents the mean ± standard deviation of three or more biological replicates, and asterisks indicate significant difference compared with WT (Student's t test, \*\*P < 0.05; ns = no significant difference).

were constructed and transiently expressed, along with 35S:eGFP as control, in susceptible grapevine "Cabernet Sauvignon" leaves via Agrobacterium-mediated transformation. The transformed leaves were inoculated with powdery mildew and stained with trypan blue at 3 dpi (days post inoculation). As shown in Supplementary Fig. S6, the

total of hyphal length of OE-WRKY10 was 790  $\mu$ m, while those of OE-WRKY30 and GFP were 480 and 670  $\mu$ m respectively. These results indicated that overexpression of VviWRKY30 in leaves increased grapevine resistance to powdery mildew, while overexpression of VviWRKY10 was just the opposite.

452

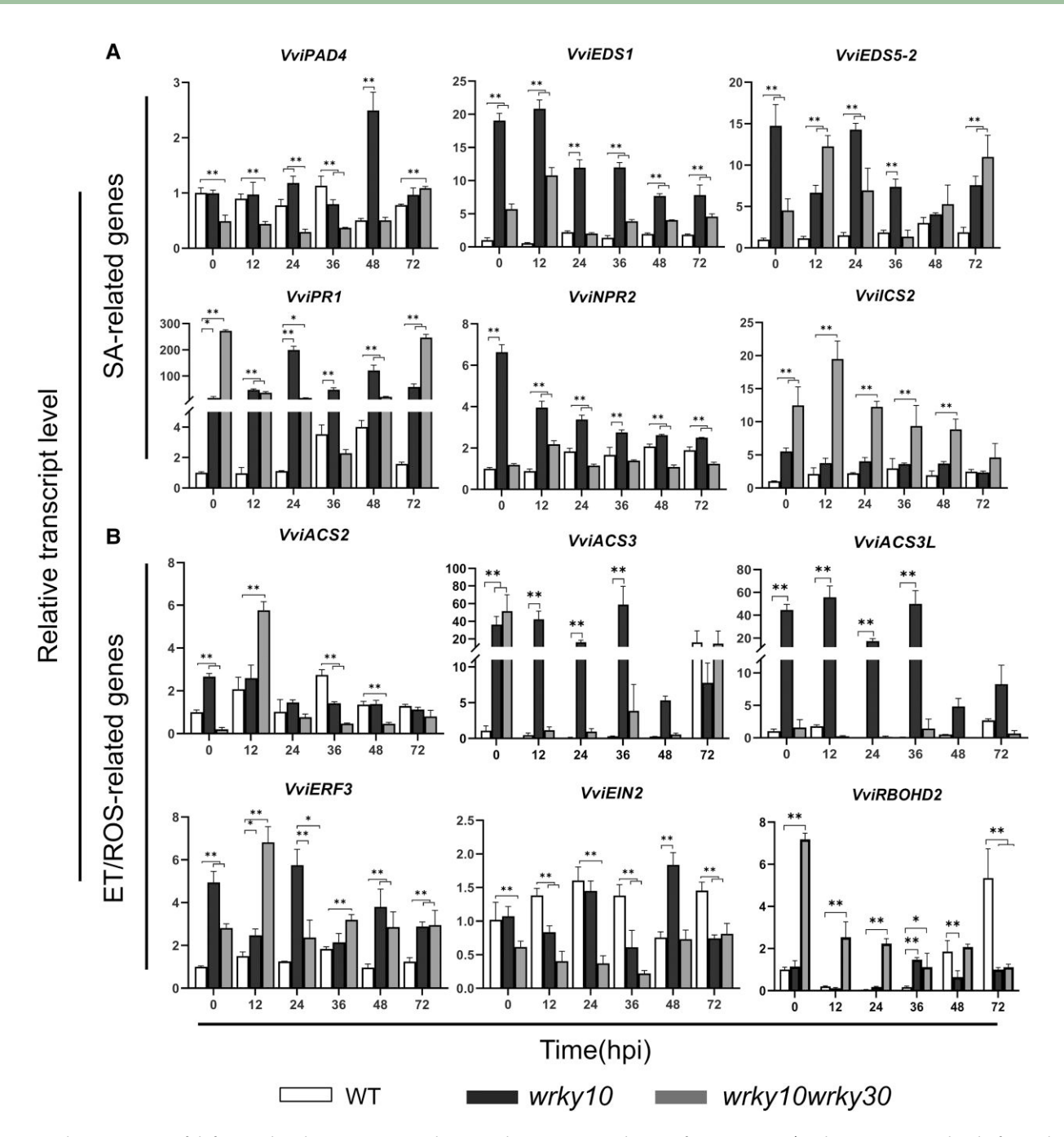


Figure 5. The expression of defense-related genes in WT and mutant lines post inoculation of En. NAFU1. A) Relative transcript level of SA-related genes. SA, salicylic acid. B) Relative transcript level of ET/ROS-related genes. ROS, reactive oxygen species; ET, ethylene. VviACTIN7 gene was used as an endogenous control. Each data point represents the mean  $\pm$  standard deviation of three biological replicates, and asterisks indicate significant difference compared with WT (GenBank accession numbers: VviPAD4 XM\_010654614.2, VviEDS1 NM\_001281038.1, VviEDS5-2 XM\_002274777.4, VviPR1 XM002273752, VviNPR2 XM\_002274009.3, VviICS2 XM\_019226638.1, VviACS2 XM\_002278453.4, VviACS3 XM\_003635528.3, VviACS3L  $XM_002269744.4$ , VviERF3  $XM_002277986.3$ , VviEIN2  $XM_002276363.3$ , VviRBOHD2  $XM_019222717.1$ .) (Two-way ANOVA, \*\*P < 0.01; \*P < 0.05).

#### Mutations in VviWRKY10 and VviWRKY30 affect gene expression in multiple defense pathways

The activation of SA, ET, and ROS pathways induced by pathogens plays a key role in plant defense. To explore changes in these pathways in mutants, some key genes were selected and measured by RT-qPCR assays in the mutant and WT leaves. As shown in Fig. 5, in wrky10, VviPAD4 was highly induced by En. NAFU1 at 48 hpi, which is 5-fold of the WT expression level, while VviEDS1, VviEDS5-2, VviPR1, VviNPR2, VviACS3, VviACS3L, and VviERF3 were always more highly expressed upon inoculation, with their peak values being 40-, 14-, 200-, 6-, 197-, 32-, and 4.7-fold of the expression levels of the WT, respectively. The transcription level of VviACS2 in wrky10 was 2.5-fold of that in

WT at 0 hpi, and there was no significant difference after inoculation, even lower than WT at 36 hpi, while expression of VviEIN2 and VviRBOHD2 peaked at 48 and 36 hpi, showing 2.6- and 9.3-fold increase compared to that in WT, respectively. In wrky10wrky30, the transcription levels of VviPAD4, VviNPR2, VviACS2 fluctuated at different time points but over all there was no significant difference compared to those of WT. Interestingly, VviEDS1, VviEDS5-2, VviPR1, VviICS2, VviERF3, and VviRBOHD2 in wrky10wrky30 exhibited higher levels upon inoculation, with their peak values being 19-, 12-, 270-, 9-, 4.8-, and 7.2-fold of the levels in WT, respectively. The expression of VviACS3 in wrky10wrky30 was 51-fold of that in WT at 0 hpi, but soon returned to the WT level after inoculation, while there was no significant difference in the expression of VviACS3L and VviEIN2 between wrky10wrky30 and WT. Collectively, the above results showed that most of the genes involved in the SA, ET, and ROS pathways in wrky10wrky30 and wrky10 in particular were significantly increased upon inoculation with En. NAFU1, which may explain the enhanced disease resistance in these mutant lines especially wrky10.

To further examine if the upregulation of the pathway genes indeed leads to increases biosynthesis of SA or ET in the mutant line, content of SA and ET in leaf tissues of WT and the mutant lines was measured prior to, 36, 72 hpi, and 14 dpi (for ET only). As expected, SA content of wrky10 and wrky10wrky30 were 6- and 3-fold of that of WT, respectively at 36 hpi; SA content of wrky10 dropped to the level of the WT and maintained at a low level, while SA content of wrky10wrky30 was still higher than that of the WT (Fig. 4E). Because leaves of wrky10 infected with powdery mildew (but not those of wrky10wrky30), often senesced earlier than those of WT (Fig. 4F, Supplementary Fig. S7), ET content in wrky10 and WT (but not the wrky10wrky30 double mutant because of their weak growth and insufficient leaf tissue for analysis; Fig. 3C) was measured prior to and at 14 dpi with En. NAFU1. The ET content in wrky10 was slightly higher (1.5-fold) than that in WT in the absence of En. NAFU1; however, the ET content in wrky10 further increased significantly upon infection by powdery mildew, reaching ~8× of that in WT at 14 dpi (Fig. 4G). These results suggested that VviWRKY10 and VviWRKY30 affected the resistance to powdery mildew by changing the accumulation of SA and ET in grapevine.

### VviWRKY10 and VviWRKY30 regulate the transcription of SA-, ET-, and ROS-related genes

WRKY TFs function mainly by binding to the W-box (TTGACC/T), a typical *cis*-acting element on the promoters of the target genes (Rushton et al. 2010). We selected genes of the SA, ET, and ROS pathways, analyzed their promoters, and found that all of them contained at least one canonical W-box (Supplementary Fig. S8A). Further, DLUC reporter assays was used to identify the relationship between VviWRKY10, VviWRKY30, and potential downstream target

genes. Different combinations of reporters and effecters, in which 35S:GFP was used as the control of the effecter and 35S:REN (Renilla luciferase) was used as an internal control (Fig. 6A), were used to co-transform N. benthamiana protoplasts, followed by measuring LUC (Firefly luciferase) and REN activities sequentially to reflect the transcriptional activity of individual promoters in vivo. As shown in Fig. 6B, compared to GFP, VviWRKY10 and VviWRKY30 inhibited promoter activities of six SA-related genes (VviICS2, VviEDS5-1, VviEDS5-2, VviPR1, VviPR5, and VviPR10.3L2), two ET-related genes (VviACS1 and VviEIN2), and one ROS-related gene (VviRBOHD2), while they had no significant effect on the promoter activity of VviACS2. Additionally, VviWRKY30 significantly enhanced promoter activities of VviNPR2, VviACS3, and VviACS3L. The results suggest that VviWRKY10 and VviWRKY30 could inhibit the promoter activities of multiple genes involved in the SA, ET, and/or ROS pathways and that VviWRKY30 may also enhance the expression of other genes in the same pathways.

### VviWRKY10 and VviWRKY30 directly bind to the promoters of SA-, ET- and ROS-related target genes

To verify whether VviWRKY10 and VviWRKY30 directly regulate SA, ET, and ROS pathways via binding to the W-boxes in the promoters of the genes whose transcription was inhibited or activated as shown above, we selected six genes VviEDS5-2, VviPR1, VviPR5, VviACS3, VviACS3L, and VviRBOHD2 for the tests by using ChIP-qPCR and EMSA. The probes and primers used in the experiment were labeled on each gene promoter (Supplementary Fig. S8B). After analyzing the cloned genes, it was found that the predicted protein sequences of VviACS3 and VviACS3L were highly conserved, differing only in one amino (Supplementary Fig. S9) in addition to their exact same W-box sequences in their promoters. Hence, the same probe and primers were used to detect VviACS3 and VviACS3L (Supplementary Figs. S8B and S9A).

First, we used grapevine callus overexpressing VviWRKY10 or VviWRKY30 for ChIP assays. As shown in Fig. 7, A to E, VviWRKY10 and VviWRKY30 were significantly enriched in fragments including F2 of ProEDS5-2, F1 of ProPR1, F2 of ProPR5, F2 of ProACS3/ACS3L, F1, and F4 of ProRBOHD2. In addition, VviWRKY10 was enriched to F3 of ProRBOHD2; VviWRKY30 was enriched to F1 of ProEDS5-2, F2 of ProPR1, and F2 of ProRBOHD2. Next, His-tagged VviWRKY10 and VviWRKY30 were expressed in E. coli and the purified proteins together with W-box-containing oligonucleotide probes were subjected to EMSA, with unlabeled and mutant probes as competitors. The results indicated that the purified VviWRKY10 or VviWRKY30 proteins could specifically bind to the W-box (Supplementary Fig. S10). Then, similar EMSA was performed using purified VviWRKY10 or VviWRKY30 proteins and labeled oligonucleotide probes synthesized based on promoter sequences enriched by both of these two

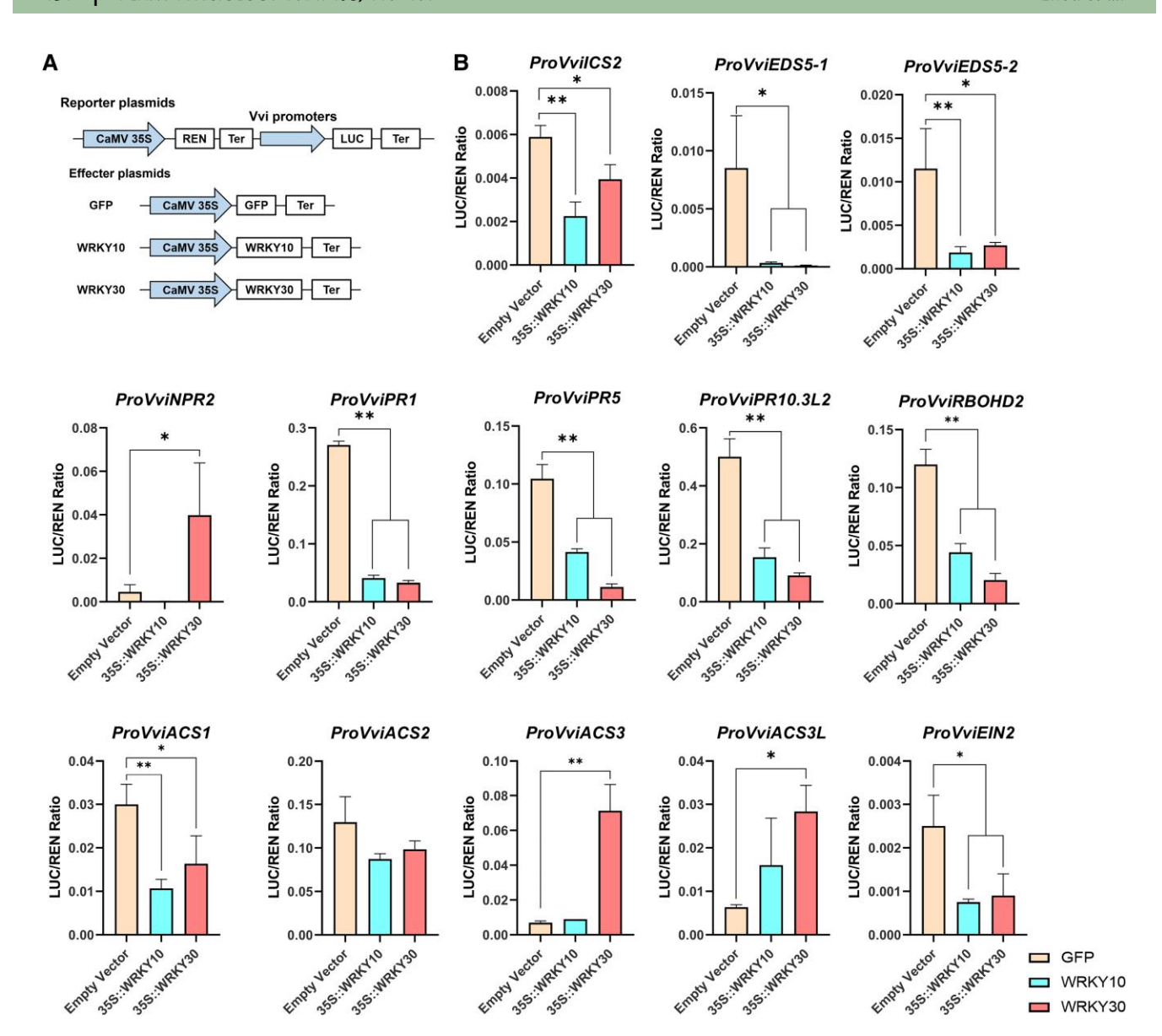


**Figure 6.** VviWRKY10 and VviWRKY30 regulate the transcription of SA-, ET-, and ROS-related genes by dual LUC reporter assays. **A)** Schematic diagram of reporter and effecter constructs used in the DLUC reporter assays. In the reporter plasmids, Renilla (REN) luciferase gene driven by CaMV35S promoter was used as the internal control, and the target gene promoters are fused to the LUC (Firefly Luciferase). In the effecter plasmids, GFP (control), WRKY10 and WRKY30 are driven by CaMV35S promoter. Ter, transcriptional terminator sequence. **B)** Dual luciferase reporter assays results. Different combinations of reporter and effecter plasmids were co-expressed in protoplast of *N. benthamiana*. The ability of WRKY10 and WRKY30 to regulate the reporter LUC gene was represented by the ratios of LUC to REN. The 35S:REN served as an internal control. Each data point represents the mean  $\pm$  standard deviation of three biological replicates, and asterisks indicate significant difference compared with GFP (Student's t test, \*\*P < 0.05).

proteins, with unlabeled sequences as competitors. The results showed that both VviWRKY10 and VviWRKY30 could form protein–probe complex hysteresis bands with the labeled probes, and the bands were substantially weakened when the unlabeled probes were present (Fig. 7, F to J). Thus, results from our in vivo and in vitro experiments consistently demonstrated that VviWRKY10 and VviWRKY30 could directly bind to the promoters of *VviEDS5-2*, *VviPR1*, *VviPR5*, *VviACS3/ACS3L*, and *VviRBOHD2*.

### VviWRKY10 and VviWRKY30 directly bind to mutual promoters and inhibit expression

It was reported that AtWRKY18 and AtWRKY40 physically associate with each other in A. thaliana (Xu et al. 2006). In order to explore whether VviWRKY10 and VviWRKY30 interact with each other, we first measured the mRNA levels of VviWRKY30 in leaves of wrky10 and WT prior to and post-inoculation with En. NAFU1. As shown in Fig. 8A, at 0 hpi, the level of VviWRKY30 in wrky10 was 51-fold than that of

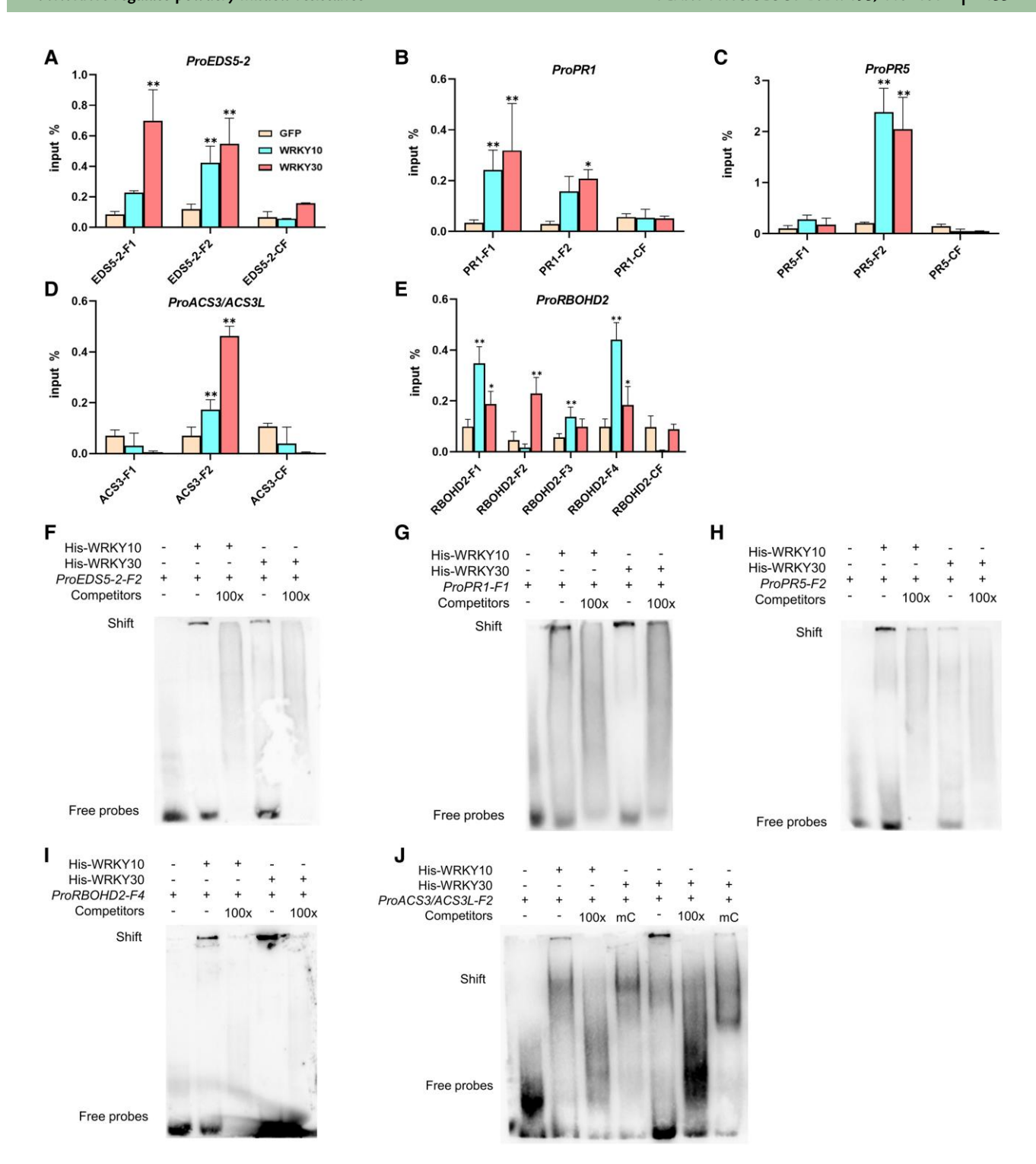


**Figure 7.** ChIP-qPCR and EMSA to examine the association between WRKY10, WRKY30 and its targets. **A to E)** Association of WRKY10 and WRKY30 with its targets by ChIP-qPCR assays. Chromatin prepared from WRKYs-GFP callus were detected with qPCR with chromatins prepared from GFP as the control. Each data point represents the mean  $\pm$  standard deviation of three biological replicates, and asterisks indicate significant difference compared with CF (F1 to F4, sequences of fragments designed from 5' to 3' WRKYs may bind; CF, fragments that WRKYs do not bind. Student's t test, \*\*P < 0.01; \*P < 0.05). **F to J)** Competitive EMSA to detect the binding of WRKY10 and WRKY30 to promoters of target genes. *VviACS3* and *VviACS3L* were used the same fragments (Supplementary Fig. S8). The DNA-binding assays were performed using purified His-WRKYs protein and biotin-labeled fragments of the promoters containing the W-boxes, using nonlabeled fragments as competitors in a molar excess of 100×. mC, mutant competitor. The specificity of bound *ProACS3/ACS3L* was further confirmed using mC (J). The + and – symbols indicate the presence and absence of components. The bands at the upper and lower part of membranes indicate shift (protein–probe complex) and unbound free probes, respectively.

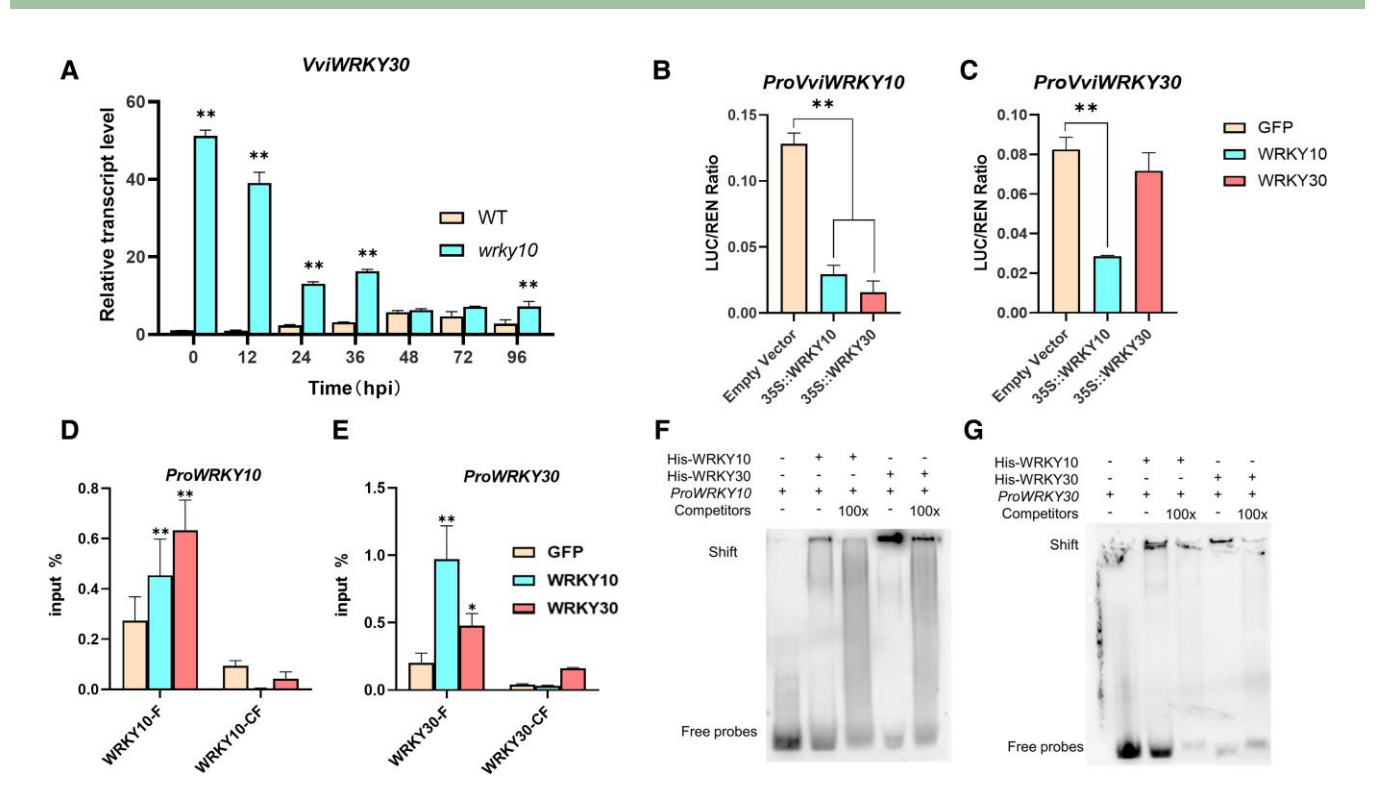


**Figure 8.** VviWRKY10 and VviWRKY30 directly bind to mutual promoters and inhibit expression. **A)** Relative transcript level of *VviWRKY30* in WT and *wrky10. VviACTIN7* gene was used as an endogenous control. **B)** WRKY10 and WRKY30 repress the expression of *VviWRKY10* by dual LUC reporter assays. **C)** WRKY10 repress the expression of *VviWRKY30* by DLUC. **D to G)** EMSA and ChIP assays of WRKY10 and WRKY30 binding to each other's promoters. Each data point represents the mean  $\pm$  standard deviation of three biological replicates, and asterisks indicate significant difference compared with WT **(A)**, GFP **(B, C)**, and CF **(D** and **E) (F,** sequences of fragments designed from 5' to 3' WRKYs may bind; CF, fragments that WRKYs do not bind; two-way ANOVA **(A)**, student's *t* test **(B** to **E)**, \*\*P < 0.01; \*P < 0.05).

WT. Although the transcript level decreased after inoculation, it was still higher than that of WT at most time points (Fig. 8A). Further, LUC assays showed that VviWRKY10 can inhibit its own and *VviWRKY30* promoter activities, which can be partially verified by the increased expression of *VviWRKY30* in *wrky10* (Fig. 8, A and B). In addition, VviWRKY30 can also inhibit the promoter activity of *VviWRKY10* (Fig. 8C). Finally, EMSA and ChIP assays further showed that VviWRKY10 and VviWRKY30 could directly bind to each other's promoters (Fig. 8, D to G). These results suggested that VviWRKY10 and VviWRKY30 may be involved in mutual inhibition of each other's transcription.

#### Discussion

WRKY TFs play important regulatory roles in defense against pathogens in plants. The Arabidopsis WRKY TFs, AtWRKY18 and AtWRKY40, act redundantly as negative regulators of basal resistance against powdery mildew in Arabidopsis (Chen and Chen 2002; Xu et al. 2006; Shen et al. 2007; Pandey et al. 2010; Abeysinghe et al. 2019). In this study, we investigated the roles of two grapevine TFs, VviWRKY10 and VviWRKY30, as putative orthologs of AtWRKY18 and AtWRKY40, in grapevine defense responses against powdery mildew. Our results have revealed complex regulatory mechanisms of these two

grapevine TFs that are distinct from the relatively simple functional redundancy of their Arabidopsis putative orthologs.

In an early study, Pandey et al. proposed that the adapted powdery mildew pathogen Golovinomyces orontii alters the balance of the SA pathway and the JA pathway via impacting the functionally redundant AtWRKY18/40 in Arabidopsis during early infection, thereby subverting host defense (Pandey et al. 2010). Our study found that VviWRKY10 and VviWRKY30 may play distinct roles in different stages of E. necator infection. VviWRKY10 was induced in an early stage of infection, while VviWRKY30 was induced at a later time, implying differential roles in transcriptional regulation of host defense (Fig. 1, B and C). Consistently, E. necator-induced ROS and callose accumulation in wrky10 were significantly increased compared with those in the WT, which corresponds with a significant reduction of hyphal growth in leaves of wrky10 compared to that of the WT (Fig. 4, A to D), supporting a role of VviWRKY10 in negative regulation of defense against powdery mildew. Interestingly, even though in the wrky10wrky30 double mutant also showed enhanced resistance to the pathogen, the level of resistance was lower than that of wrky10, and there was considerable mycelium growth (Fig. 4, Table 1), implying a complex and perhaps antagonistic relationship between VviWRKY10 and VviWRKY30. Indeed, while transient overexpression of VviWRKY10 in grapevine

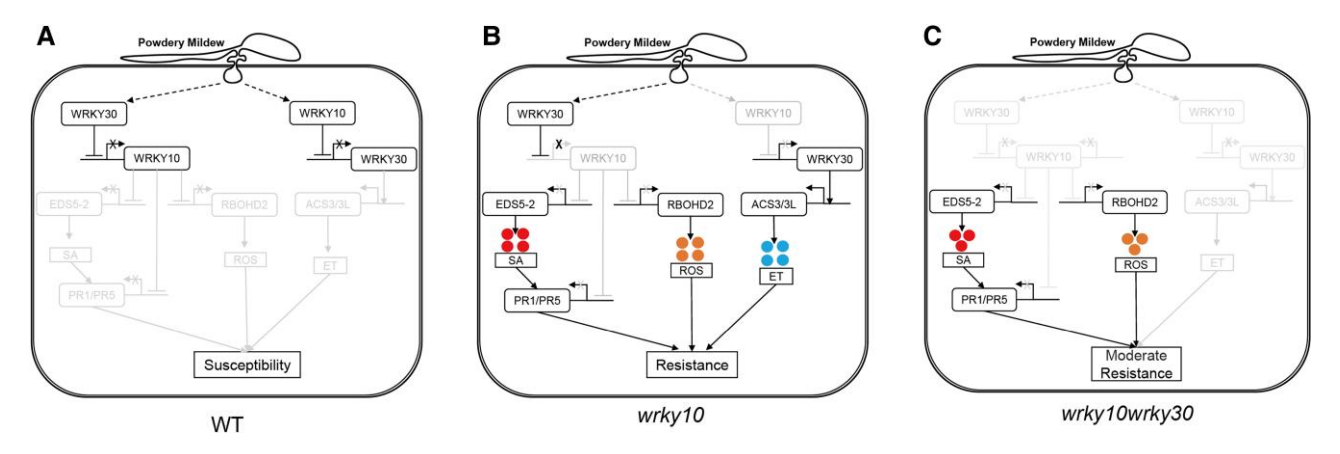


**Figure 9.** A proposed model of two grapevine transcription factors (WRKY10 and WRKY30) in regulating powdery mildew resistance. **A)** In WT, WRKY10 and WRKY30 inhibited each other and both downstream pathways were inhibited, susceptible to powdery mildew. **B)** In *wrky10*, the SA and ROS pathways were activated, and WRKY30 activated the ET pathway, resulting in resistance to powdery mildew. **C)** In *wrky10wrky30*, only SA and ROS pathways were activated, resulting in moderate resistance to powdery mildew. SA, salicylic acid; ROS, reactive oxygen species; ET, ethylene. Spheres represent SA, ROS, and ET, respectively, from left to right.

leaves led to significantly increased hyphal length of *En.* NAFU1, transient overexpression of VviWRKY30 did the opposite (Supplementary Fig. S6), further suggesting that VviWRKY10 and VviWRKY30 play opposing roles in modulating defense against powdery mildew in grapevine.

Given that plants adopt contrasting strategies to fight against biotrophic and necrotrophic pathogens, our results on *VviWRKY10* are consistent with and provide further explanations for the earlier observation that overexpression of *VaWRKY10* in *V. vinifera* cv. Thompson Seedless substantially improved resistance to *B. cinerea*, a necrotrophic fungal pathogen (Wan et al. 2021). Specifically, we found that the enhanced resistance to powdery mildew in the *wrky10* single mutant was associated with the activation of SA, ET, and ROS pathways (Figs. 4 and 5).

Notably, our results on VviWRKY30 also largely agree with the results of an earlier study where VviWRKY30 (named as VviWRKY40 in that study) was reported to play a role in PvRXLR111-mediated suppression of flg22-induced ROS production, thereby promoting *Phytophthora capsici* infection (Ma et al. 2021). Our study provides more mechanistic insight onto how VviWRKY30 works: VviWRKY30 binds to the VviRBOHD2 promoter and inhibit its expression. This conclusion was supported by our genetic evidence that loss of VviWRKY30 in the wrky10wrky30 double mutant resulted in increased VviRBOHD2 expression (Figs. 5B, 6B, and 7, D and 1). Furthermore, we found that increased expression of VviWRKY30 in the wrky10 mutant may be attributable to the increased expression of VviACS3 and VviACS3L genes, thereby activating the ET pathway (Figs. 6B and 7, E and J), which in turn may partially explains the enhanced resistance to En. NAFU1 at later stages of infection (Figs. 4G, 5B, and 8A).

It is well known that WRKYs usually play roles in transcriptional regulation of plant defense (Eulgem and Somssich 2007). For example, it has been shown that AtWRKY18 and

AtWRKY40 directly bind to the promoters of multiple genes acting in the SA, ET and JA pathways, directly regulating their transcription, resulting in the formation of a complex regulatory network (Birkenbihl et al. 2017). In this study, using DLUC, ChIP, and EMSA assays, we demonstrated that VviWRKY10 can directly bind to the promoters of EDS5-2, PR1, PR5, RBOHD2, and WRKY30 and inhibit the expression of these target genes, thereby inhibiting the accumulation of SA and ROS, and the WRKY30 protein (Figs. 6B, 7, A to D, F to I, and 8, C, E and G). Intriguingly, we also showed that VviWRKY30 can directly bind to the promoter of VviWRKY10, inhibiting its expression and downregulating the SA pathway at an early stage of infection while promoting the ET pathway for limiting infection at a later stage (Figs. 6B, 7, E and J, and 8, B, D, and F).

Based on the results from this study, we propose a working model for the role of VviWRKY10 and VviWRKY30 in the regulation of powdery mildew resistance in grapevine (Fig. 9). Specifically, we propose: (i) VviWRKY10 inhibits the expression of VviEDS5-2, VviPR1, VviPR5, and VviRBOHD2, presumably to avoid overactivation of the SA-dependent defense responses upon powdery mildew infection in grapevine; (ii) VviWRKY30 promotes the expression of VviACS3 and VviACS3L to increase ET production for limiting powdery mildew growth at a later stage of infection; and (iii) VviWRKY10 can inhibit VviWRKY30 accumulation to inhibit ET synthesis, while VviWRKY30 can also inhibit VviWRKY10 accumulation to promote production of SA and ROS. It is possible that the distinct roles of VviWRKY10 and VviWRKY30 together with their mutual inhibition are required for the activation of measured and balanced defenses involving multiple hormonal pathways against powdery mildew and likely other pathogens in grapevine.

#### Materials and methods

#### Plant materials and growth conditions

The WT grapevine (*V. vinifera* cv. Cabernet Sauvignon) and transgenic plantlets were cultured under the same conditions. In April and May of 2021, we observed the phenotypes of WT, *wrky10*, and *wrky10wrky30* mutant plants in chambers with temperature ranging from 22 to 27 °C, relative humidity ranging from 75% to 90%, and under a long-day photoperiod (16 h:8 h, light (200  $\mu$ mol m<sup>-2</sup> s<sup>-1</sup>):dark). From May 2021 to November 2023, the WT and mutant plants were transplanted in a greenhouse with temperature ranging from 25 to 35 °C (in summer) or 5 to 25 °C (in winter), relative humidity ranging from 40% to 75%.

#### Cloning and sequence analysis

The *VviWRKY10* and *VviWRKY30* genes were amplified from "Cabernet Sauvignon" leaf cDNA using Planta Max Super-Fidelity DNA Polymerase (Vazyme Bio Co., Nanjing, China). The amplified sequences were integrated into the pMD-19T vector and then introduced into *E. coli* DH5α. Ten clones of each gene were randomly selected and sequenced. The amplification primers were designed according to the genome database of *V. vinifera* cv. Pinot Noir in the NCBI database (https://www.ncbi.nlm.nih.gov/). The sequences of amplified primers are shown in Supplementary Table S1.

The coding sequences of *VviWRKY10* and *VviWRKY30* genes obtained by sequencing were translated into protein sequences by DANMAN, and then BLAST-P search was performed in NCBI. The genes with the highest similarity to *VviWRKY10* and *VviWRKY30* in other species were selected, and the phylogenetic tree was constructed by MEGA-X. The parameters were set as follows: bootstrap value was 1,000, p-distance model was selected, partial deletion value was 50, and other default settings. The protein sequences of VviWRKY10, VviWRKY30 and AtWRKY18, AtWRKY40 and AtWRKY60 were analyzed by Jalview, and the parameters were set by default.

#### Subcellular location assays

The coding sequences of *VviWRKY10* and *VviWRKY30* were amplified and ligated into the pCAMBIA2300 vector, which contains a 35S promoter and a C-terminal GFP tag. The recombinant vectors and 35S:AtH2B-mCherry fusion expression vector were transformed into *N. benthamiana* leaves, respectively, combined. Fluorescence photos were taken using a confocal laser scanning microscope (LEICA TCS SP8, Germany) 3 d after transfection. The filter settings are Ex 488 nm/Em 498 to 545 nm for GFP and Em 670 to 720 nm for Chl.

#### Target selection and vector construction

In the genome of "Pinot Noir", VviWRKY10 gene is located on chromosome 4, 2,201 bp in length, encoding 296 amino acids. VviWRKY30 gene is located on chromosome 9, the

full length of 1,561 bp, encoding 311 amino acids. Select target points according to design principles (Xing et al. 2014). Based on the NCBI database, BLAST-P search was performed on the target sequences using the "Pinot Noir" genome to ensure the specificity of the target sites selection. At the same time, the amplified VviWRKY10 and VviWRKY30 were compared to ensure that the selected target sites were completely consistent in "Cabernet Sauvignon". According to the sequence of vector pKSE401-GFP and intermediate vector pCBC-DT1T2, specific primers containing Bsa I restriction site were designed. The pCBC-DT1T2 plasmid was used as a template for PCR amplification using Planta Max Super-Fidelity DNA Polymerase to obtain two sgRNA expression cassettes. The purified PCR products were assembled into the pKSE401-GFP vector. The primers are shown in Supplementary Table S1.

#### Plant transformation and detection of mutations

The grapevine PEM was transformed by A. tumefaciensmediated genetic transformation (Wan et al. 2020). Using stereomicroscope (MZ10F, LEICA, Germany) to observe whether the plantlets with GFP fluorescence, screening transgenic positive plants. The 0.5 to 1.0 g leaves of regenerated positive "Cabernet Sauvignon" plantlets were taken, and the whole gDNA was extracted by CTAB method. Gene-specific primers were used to amplified the positive plants across the target region and recovered the PCR products for sequencing. DNA sequence alignment was performed on the sequencing results to determine whether editing occurred, and then the editing type was analyzed by "DSDecodeM" (Liu et al. 2015). For the edited plants whose "DSDecodeM" decoding failed, the PCR purified product was cloned into pMD19-T, and 10 single clones were randomly selected for Sanger sequencing to analyze the editing type. Multiple sequence alignment and amino acid sequence analysis were performed using Jalview to determine the effect of each gene mutation type on amino acids. The primers are shown in Supplementary Table S1.

#### Evaluation of resistance to powdery mildew

In order to explore the phenotype of wrky10 single mutant and wrky10wrky30 double mutant after powdery mildew infection, the leaves of the mutants and WT were inoculated with En. NAFU1 (Gao et al. 2016). The leaves were stained with trypan blue at 3 dpi, DAB, and aniline blue at 5 dpi to observe the growth of powdery mildew and the cell reaction of grapevine leaves (Hu et al. 2018, 2019). At the same time, the inoculated leaves were frozen for RT-qPCR and hormone measuring after inoculation.

### Agrobacterium-mediated transient expression in grapevine leaves

For transient overexpression of *VviWRKY10* and *VviWRKY30*, the coding sequences of these two genes were translationally in-frame fused with eGFP in the binary vector pCAMBIA2300

(digested with BamH I and Kpn I) under control of the 35S promoter via homologous recombination. The resulting 35S:VviWRKY10-eGFP and 35S:VviWRKY30-eGFP, as well as 35S:eGFP DNA constructs were introduced into Agrobacterium tumefaciens strain GV3101. Agrobacterial cells were grown to  $OD_{600} = 0.5$  to 0.6, spun down at 4,000 rpm for 5 min, and resuspended in an equal volume of buffer (0.5% (w/v) glucose, 50 mm MES (pH 5.6), 3 mm  $Na_2HPO_4$ , 100  $\mu$ M acetosyringone). After incubation at 28 °C for 1 h, the resuspended bacterial solution was injected via the leaf abaxial side into the third to fifth fully expanded "Cabernet Sauvignon" leaves. Two days later, the infiltrated leaves were inoculated with En. NAFU1. At 3 dpi, Trypan blue was used to visualize fungal structures and hyphal lengths were measured with the aid of an Olympus BX-63 microscope (Japan).

#### RNA extraction and RT-qPCR assays

The leaves of "Cabernet Sauvignon" were inoculated with En. NAFU1. The leaves were collected at 0, 12, 24, 36, 48, 72, and 96 hpi. At 12Mhpi, parts of five to seven inoculated leaves were randomly cut for RNA sample collection, and trypan blue staining was performed to check spore germination. After spore germination, five leaf pieces (~100 mg) were randomly collected at each time point as one leaf sample for RNA extraction using the E.Z.N.A. Plant RNA Kit (Omega, Guangzhou, China). About 1  $\mu$ g RNA was used for cDNA synthesis using HiScript Q Select RT SuperMix (Vazyme, Nanjing, China). The cDNA samples served as template for qPCR for measuring mRNA levels of the selected defense genes and VviACTIN7 (XM\_002282480.4) as internal control. The relative transcription level of the defense genes was calculated with the  $2^{-\Delta Ct}$  method. The expression level for each gene was presented as the mean value of three biological replicates, and significance testing was performed by two-way ANOVA. The sequences of the primers used for RT-qPCR are listed in Supplementary Table S1.

#### Hormone measurements

Taken leaves at 0, 36, and 48 hpi, 0.1 g was weighed and put into 2 mL sterile centrifuge tubes, sterilized steel beads were added, and quickly frozen in liquid nitrogen. The leaves were fully ground with a tissue grinding instrument, and 1 mL of ethyl acetate extract was added. After fully mixing for 10 min, centrifuged at 10,000 rpm, 4 °C for 5 min, the supernatant was transferred to new centrifuge tubes. The organic phase in the centrifuge tube was blown dry with a nitrogen blowing instrument, and 200  $\mu$ L 50% methanol (v/v) solution was added to fully shake and mix. After centrifugation at 10,000 rpm for 5 min, the supernatant was absorbed with a 1 mL syringe, and filtered into a liquid injection bottle using 0.22  $\mu$ m organic filters.

The leaves at 0 and 14 dpi were made into leaf discs. Twenty leaves in each group were randomly selected in 10 mL headspace bottles, sealed in the incubator for 36 h,

and 1 mL of gas was extracted to determine ET by gas chromatography, were calculated by standard curve method.

The quantitative analysis of each hormone and ET content were performed using the standard curve method.

### Promoter analysis and dual luciferase reporter assays (DLUC)

The DNA sequence of 2,000 bp upstream of the start codon of *VviWRKY10, VviWRKY30*, SA-, ET-, and ROS-related genes were selected for DLUC assays. Gene Regulation (gene-regulation. com) and PlantCARE, a database of plant promoters and their *cis*-acting regulatory elements (bioinformatics.psb.ugent.be/webtools/plantcare) were used to predict *cis*-acting elements such as W-boxes from the selected promoter sequences. The diagrams showing the *cis*-acting elements of the analyzed genes were drawn by Gene Structure Display Server (gsds.gao-lab. org).

The coding sequences of *VviWRKY10* and *VviWRKY30* were amplified and ligated into the pBI221-GFP (digested with Xba I and Xho I) vector as effecters, the promoters of defense-related gene were inserted into the 35S-Rluc-35S-Fluc vector (digested with Hind III and Nco I) as reporters. According to the previous method, different combinations of reporter and effecter plasmids were co-expressed in *N. benthamiana* protoplast (Zhao et al. 2016). Full-wavelength microplate reader (Infinite M200pro, Tecan, Switzerland) for detection, and calculation of relative transcriptional activity based on LUC to REN ratio.

#### **EMSA**

The coding sequences of *VviWRKY10* and *VviWRKY30* were amplified and cloned into pET30a vector (digested with BamH I and Kpn I). The His-WRKY10 and His-WRKY30 fusion protein were expressed in *E.coli* strain Rosetta (DE3). The fusion protein was induced by 0.2 mm IPTG and purified by protein purification instrument (NGC Discover 10). Complete the EMSA experiment according to the Chemiluminescent EMSA Kit instructions (Beyotime, China). Labeled probes, unlabeled probes, and mutant probes sequences are shown in Supplementary Table S1.

#### ChIP-qPCR assays

grapevine transgenic callus stably expressing VviWRKY10-GFP or VviWRKY30-GFP were used as materials. One gram of callus was cross-linked with 1% formaldehyde (v/v) for 15 min, and then glycine with a final concentration of 100 mm was added to terminate the reaction, washed twice with distilled water and frozen in liquid nitrogen. Next, the chromatin was treated with ultrasound and the DNA fragments were precipitated using GFP-TRAP Magnetic Agarose beads (Chromotek, gtma-20). After protein digestion, the precipitated DNA was purified and directly used as qPCR template. The transformed GFP empty callus was used as the negative control, and the DNA without magnetic beads precipitation was used as input. The results are presented as a percentage of input. Sequences at least

600 bp after the translation initiation site were used as controls. The primers are shown in Supplementary Table S1.

#### Statistical analysis

All variance tests were performed using GraphPad Prism 8. In this paper, two-way ANOVA was used for all gene expression analysis (Figs. 1, B and C, 5, and 8A) and Student's t test was used for the rest experiments. Asterisks above columns indicate significant differences (\*\* = P < 0.01; \* = P < 0.05; ns = no significant difference).

#### **Accession numbers**

Sequence data from this article can be found in the GenBank/ EMBL data libraries under accession numbers NP\_001312010.1, NP\_001409692.1, XP\_008342807.1, NP\_178199.1, NP\_567882.1, NP\_180072.1, PP236376, and PP236377.

#### Acknowledgments

We thank Dr. Wei Rong of Hainan University for kindly providing pET30a vector, and Dr. Kunming Chen of Northwest A&F University for kindly providing 35S-Rluc-35S-Fluc vector. The authors would like to thank the anonymous reviewers for their comments on the manuscript.

#### **Author contributions**

Y.Q.W. conceived the study with help from S.X.; M.Z., H.Y.W. performed the experiments; X.N.Y., K.C.C., and Y.H. conducted data analysis; M.Z. wrote the manuscript; and Y.Q.W. and S.X. revised the manuscript. All of the authors read and approved the final manuscript.

#### Supplementary data

The following materials are available in the online version of this article.

**Supplementary Figure S1.** Protein structure analysis of VviWRKY10 and VviWRKY30.

**Supplementary Figure S2.** Genetic transformation and fluorescence detection of regenerated plants.

**Supplementary Figure S3.** Statistics of regenerated plants. **Supplementary Figure S4.** Sequencing chromatograms of regenerated plants.

**Supplementary Figure S5.** ABA and IAA contents in WT and mutants.

**Supplementary Figure S6.** Transient overexpression of *VviWRKY10* and *VviWRKY30* altered resistance to *En*. NAFU1 in *V. vinifera*.

**Supplementary Figure S7.** Phenotypes of WT and *wrky10* lines 14 dpi of *En.* NAFU1.

**Supplementary Figure S8.** Schematic diagram of promoters of related genes.

**Supplementary Figure S9.** Alignment of promoter and protein sequences of *VviACS3* and *VviACS3L* genes.

**Supplementary Figure \$10.** Validation of VviWRKY10 and VviWRKY30 binding W-box ability.

**Supplementary Table S1.** Primers used in this study.

#### **Funding**

This work was supported by the National Natural Science Foundation of China (Grant No. 32272670, 31972986) to Y.Q.W. and National Science Foundation (Grant No. IOS-1901566) to S.X.

Conflict of interest statement. All authors declare no conflicts of interest.

#### **Data availability**

The data underlying this article are available in the article and in its online supplementary material.

#### References

- Abeysinghe JK, Lam K-M, Ng DW-K. Differential regulation and interaction of homoeologous WRKY18 and WRKY40 in Arabidopsis allotetraploids and biotic stress responses. Plant J. 2019:97(2):352–367. https://doi.org/10.1111/tpj.14124
- **Birkenbihl RP, Kracher B, Roccaro M, Somssich IE**. Induced genomewide binding of three arabidopsis WRKY transcription factors during early MAMP-triggered immunity. Plant Cell. 2017:**29**(1):20–38. https://doi.org/10.1105/tpc.16.00681
- Chen C, Chen Z. Potentiation of developmentally regulated plant defense response by AtWRKY18, a pathogen-induced Arabidopsis transcription factor. Plant Physiol. 2002:129(2):706–716. https://doi.org/10.1104/pp.001057
- Dang F, Wang Y, She J, Lei Y, Liu Z, Eulgem T, Lai Y, Lin J, Yu L, Lei D, et al. Overexpression of CaWRKY27, a subgroup lle WRKY transcription factor of *Capsicum annuum*, positively regulates tobacco resistance to *Ralstonia solanacearum* infection. Physiol Plant. 2014:150(3): 397–411. https://doi.org/10.1111/ppl.12093
- **Eulgem T, Somssich IE.** Networks of WRKY transcription factors in defense signaling. Curr Opin Plant Biol. 2007:**10**(4):366–371. https://doi.org/10.1016/j.pbi.2007.04.020
- Gadoury DM, Cadle-Davidson L, Wilcox WF, Dry IB, Seem RC, Milgroom MG. Grapevine powdery mildew (*Erysiphe necator*): a fascinating system for the study of the biology, ecology and epidemiology of an obligate biotroph. Mol Plant Pathol. 2012:13(1):1–16. https://doi.org/10.1111/j.1364-3703.2011.00728.x
- Gao YR, Han YT, Zhao FL, Li YJ, Cheng Y, Ding Q, Wang YJ, Wen YQ. Identification and utilization of a new *Erysiphe necator* isolate NAFU1 to quickly evaluate powdery mildew resistance in wild Chinese grapevine species using detached leaves. Plant Physiol Biochem. 2016:**98**:12–24. https://doi.org/10.1016/j.plaphy.2015.11.
- Guo C, Guo R, Xu X, Gao M, Li X, Song J, Zheng Y, Wang X. Evolution and expression analysis of the grape (*Vitis vinifera* L.) WRKY gene family. J Exp Bot. 2014:65(6):1513–1528. https://doi.org/10.1093/jxb/eru007
- **Hu Y, Gao Y-R, Yang L-S, Wang W, Wang Y-J, Wen Y-Q.** The cytological basis of powdery mildew resistance in wild Chinese *Vitis* species. Plant Physiol Biochem. 2019:**144**:244–253. https://doi.org/10.1016/j.plaphy.2019.09.049
- Hu Y, Li Y, Hou F, Wan D, Cheng Y, Han Y, Gao Y, Liu J, Guo Y, Xiao S, et al. Ectopic expression of Arabidopsis broad-spectrum resistance gene *RPW8.2* improves the resistance to powdery mildew in grape-vine (*Vitis vinifera*). Plant Sci. 2018:267:20–31. https://doi.org/10.1016/j.plantsci.2017.11.005
- Jaillon O, Aury J-M, Noel B, Policriti A, Clepet C, Casagrande A, Choisne N, Aubourg S, Vitulo N, Jubin C, et al. The grapevine genome sequence suggests ancestral hexaploidization in major angiosperm phyla. Nature. 2007:449(7161):463–467. https://doi.org/10.1038/nature06148

- Jiang J, Ma S, Ye N, Jiang M, Cao J, Zhang J. WRKY transcription factors in plant responses to stresses. J Integr Plant Biol. 2017:59(2): 86-101. https://doi.org/10.1111/jipb.12513
- **Liu W, Xie X, Ma X, Li J, Chen J, Liu Y-G.** DSDecode: a web-based tool for decoding of sequencing chromatograms for genotyping of targeted mutations. Mol Plant. 2015:**8**(9):1431–1433. https://doi.org/10.1016/j.molp.2015.05.009
- Liu X, Zhou X, Li D, Hong B, Gao J, Zhang Z. Rose WRKY13 promotes disease protection to *Botrytis* by enhancing cytokinin content and reducing abscisic acid signaling. Plant Physiol. 2022:191(1):679–693. https://doi.org/10.1093/plphys/kiac495
- Ma T, Chen S, Liu J, Fu P, Wu W, Song S, Gao Y, Ye W, Lu J. *Plasmopara viticola* effector PvRXLR111 stabilizes VvWRKY40 to promote virulence. Mol Plant Pathol. 2021:**22**(2):231–242. https://doi.org/10.1111/mpp.13020
- Pandey SP, Roccaro M, Schön M, Logemann E, Somssich IE. Transcriptional reprogramming regulated by WRKY18 and WRKY40 facilitates powdery mildew infection of Arabidopsis. Plant J. 2010:64(6): 912–923. https://doi.org/10.1111/j.1365-313X.2010.04387.x
- Raffeiner M, Üstün S, Guerra T, Spinti D, Fitzner M, Sonnewald S, Baldermann S, Börnke F. The Xanthomonas type-III effector XopS stabilizes CaWRKY40a to regulate defense responses and stomatal immunity in pepper (Capsicum annuum). Plant Cell. 2022:34(5): 1684–1708. https://doi.org/10.1093/plcell/koac032
- Rushton PJ, Somssich IE, Ringler P, Shen QJ. WRKY transcription factors. Trends Plant Sci. 2010:15(5):247–258. https://doi.org/10.1016/j.tplants.2010.02.006
- Shen Q-H, Saijo Y, Mauch S, Biskup C, Bieri S, Keller B, Seki H, Ulker B, Somssich IE, Schulze-Lefert P. Nuclear activity of MLA immune receptors links isolate-specific and basal disease-resistance responses. Science. 2007;315(5815):1098–1103. https://doi.org/10.1126/science.1136372

- **Tsuda K, Somssich IE.** Transcriptional networks in plant immunity. New Phytol. 2015:**206**(3):932–947. https://doi.org/10.1111/nph. 13286
- Wan D-Y, Guo Y, Cheng Y, Hu Y, Xiao S, Wang Y, Wen Y-Q. CRISPR/Cas9-mediated mutagenesis of *VvMLO3* results in enhanced resistance to powdery mildew in grapevine (*Vitis vinifera*). Hortic Res. 2020:**7**(1):116. https://doi.org/10.1038/s41438-020-0339-8
- Wan R, Guo C, Hou X, Zhu Y, Gao M, Hu X, Zhang S, Jiao C, Guo R, Li Z, et al. Comparative transcriptomic analysis highlights contrasting levels of resistance of *Vitis vinifera* and *Vitis amurensis* to *Botrytis cinerea*. Hortic Res. 2021:8(1):103. https://doi.org/10.1038/s41438-021-00537-8
- Wang Y, Cui X, Yang B, Xu S, Wei X, Zhao P, Niu F, Sun M, Wang C, Cheng H, et al. WRKY55 transcription factor positively regulates leaf senescence and the defense response by modulating the transcription of genes implicated in the biosynthesis of reactive oxygen species and salicylic acid in Arabidopsis. Development. 2020:147(16): dev189647. https://doi.org/10.1242/dev.189647
- Xing H-L, Dong L, Wang Z-P, Zhang H-Y, Han C-Y, Liu B, Wang X-C, Chen Q-J. A CRISPR/Cas9 toolkit for multiplex genome editing in plants. BMC Plant Biol. 2014:14(1):327. https://doi.org/10.1186/s12870-014-0327-y
- **Xu X, Chen C, Fan B, Chen Z.** Physical and functional interactions between pathogen-induced Arabidopsis WRKY18, WRKY40, and WRKY60 transcription factors. Plant Cell. 2006:**18**(5):1310–1326. https://doi.org/10.1105/tpc.105.037523
- Zhao F-L, Li Y-J, Hu Y, Gao Y-R, Zang X-W, Ding Q, Wang Y-J, Wen Y-Q. A highly efficient grapevine mesophyll protoplast system for transient gene expression and the study of disease resistance proteins. Plant Cell Tissue Organ Culture. 2016:125(1):43–57. https://doi.org/10.1007/s11240-015-0928-7